Synthesis and characterization of multiwall carbon nanotube reinforced yttria stabilized zirconia composites

Soukaina Lamnini

Ph. D. dissertation

Supervisors:
Dr. Csaba Balázsi
Dr. Katalin Balázsi

Óbudai Egyetem

Doctoral School of Materials science and Technology
Óbuda University

Thin Film Physics Department
Institute of Technical Physics and Materials Science
Centre for Energy Research

Budapest, 2020

1. Introduction

Due to their great potential and unique properties, ceramic matrix nanocomposites (CMCs) affords a new generation of technical application with excellent efficiency. Although CMCs possess various interesting properties, they often present a brittle behavior at the monolithic state, which constitutes a major issue. To overcome this issue, several attempts have been developed to improve the fracture behavior of CMCs and maintain all the other advantages of the monolithic ceramics. Zirconia (ZrO_2) based materials are one of the most widely investigated and technologically powerful ceramic materials involved in several fields. The important properties of zirconia based composites as high ionic conductivity, high mechanical strength, and stability at high-temperatures enabled their wide use in tremendous structural and multifunctional applications including: solid oxide fuel cells (SOFCs), oxygen sensors, ceramic membrane oxygen separation technology, thermal barrier coatings (TBCs) destined for high-temperature applications such as modern gas turbine, hot structure (aerospace), combustor engine components (seals, valves, and pump impellers), and refractory material. However, although the great effort and progress that have been made over the past ten years in the development of the zirconia based composites, only a very few new material systems and novel processing techniques have been discovered. Nowadays, multiwall carbon nanotube (MWCNT) reinforced ZrO_2 composites are attracting growing interest, thanks to their ability of self-healing of the crack and the possibility to tailor the desired nanostructured properties. Therefore, to completely benefit from their outstanding properties, a deep understanding of the materials' behavior across length scales was required.

The aim of my PhD work was the experimental synthesis of 8mol% yttria stabilized zirconia (8YSZ) containing 1, 5 and 10 wt% MWCNTs. I also have aimed to explore how the microstructure affect their mechanical and tribological properties. Furthermore, thesis reported on the composites ability of self-healing by limiting the crack propagation (toughening mechanism) and on the critical role of milling and SPS sintering process in the control of the grain size, phase evolution and MWCNT dispersion. The PhD work are based on the following aims and motivations:

- **Synthesis of 8YSZ containing 1, 5 and 10 wt% MWCNTs** and analysing the critical role of milling conditions and spark plasma sintering process in the control of the grain size, density and MWCNT dispersion.
- **Analysing and characterizing of the MWCNT direct and indirect effect** on the microstructure and further on the sintered 8YSZ / MWCNT composites at 1400 °C.
- **Qualitative and quantitative examinations** to reveal the composites phase evolution at powder and sintered states and to further discern whether SPS process has affected MWCNT structure and integrity with respect to its concentration.
- **Evaluation of composite´s mechanical properties,** mainly Vickers hardness, indentation fracture toughness and 3-p bending testes.
- Analysing the composites **ability of self-healing** by limiting the crack propagation (toughening mechanism) with respect to MWCNT content after surface indentation and fractographic test.
- **A new interpretation of the complex wear mechanism** reported in 8YSZ / MWCNT composites has been well outlined in function of MWCNT content, wear conditions and the variation of the applied sliding speed.
- **Understanding the complex wear mechanisms** observed in the studied composites at low V1= 0.036 m/s and high V2= 0.11 m/s sliding speeds, dry sliding conditions based on analytical studies involving SEM and EDS investigations inside and outside the wear track.

Based on the obtained results, the studied composites can be extended towards technical applications where low wear rate associated with good strength and resistant to crack propagation are essential.

2. Materials and methods

2.1 Materials, powder processing and spark plasma sintering

The powder matrix consisted of commercially available 8 mol% yttria stabilized zirconia (8YSZ, Sulzer Metco AMDRY 6643) with an average grain size of

40 μm. MWCNTs (Nanocyl) with average walls number of eight, inner/outer diameter of 3.8 nm / 9.13 nm and average length of 1.5 μm prepared by catalytic chemical vapor deposition (CCVD) process have been added to 8YSZ matrix with different addition (1, 5 and 10 wt%) (Tab. 1). The composites were milled using high efficiency attrition milling (Union Process, type 01-HD/HDDM) for 5h running at a velocity of 4000 rpm using 130 g ethanol and 280 ml zirconia balls (each of 1 mm diameter). The obtained milled slurry was then dried at 172 °C for 25 minutes and sieved by 100 μm mesh. After powder processing, the consolidation of composite powder was assessed by spark plasma sintering (SPS, HD P5 equipment FCT GmbH) at 1400 °C and uniaxial pressure of 50 MPa maintained during sintering cycle with a dwell time of 5 min. The final sintered disk composites size was 30 mm in diameter with a thickness of 5 mm.

Tab. 1. *Percentage of 8YSZ and MWCNTs in ZR, ZR-1, ZR-5 and ZR-10 composites.*

Sample	8YSZ (wt%)	MWCNT (wt%)
ZR	100	0
ZR-1	99	1
ZR-5	95	5
ZR-10	90	10

2.2 Mechanical and tribological testing methods

The hardness variation throughout the sintered sample's surface diagonal with a displacement was characterized by Vickers hardness tester (LeitzWetzi AR Germany) under 19.61 N load and 30 s a dwell of time. The indentation fracture toughness (K_{IC}) was obtained using the valid equation (5) for Palmqvist crack proposed by Shetty:

$$K_{IC} = 0.0899\left(\frac{H_V.F}{4l}\right)^{0.5}$$

where *l* (mm) is the length of the crack from the indentation corner , *F* is the force, H_v is the measured Vickers hardness value. The flexural strength was determined by the 3-point bending test using INSTRON5966 apparatus a span of 20 mm and rate of 0.0083 mm/s. The analysis of the wear behavior and the friction properties has been conducted

on high temperature tribometer THT (CSM, Switzerland) using ball-on-disk technique at room temperature (25 °C, air humidity 50–65 %).

2.3 Characterization of 8YSZ / MWCNTs composites

The apparent and bulk densities of the composites were measured using Archimedes method with water as the immersion medium. The microstructural characterization of the studied composites, namely the MWCNTs dispersion, zirconia grain size and morphology after milling and sintering, surface porosity and preliminary fratographic examination were investigated by a scanning electron microscope (SEM, LEO 1540 XB). The elemental analysis was performed by Rontec Si (Li) EDS detector located in SEM and Bruker Esprit 1.9 software. The MWCNTs agglomeration and dispersion into the matrix were studied. The wear track profile, the wear mechanism and the chemical composition after the wear test were analyzed by SEM (Thermo Scientific Scios equipped with BSE detector and Oxford X-Max EDS detector). The features of the dispersed MWCNTs addition in 8YSZ matrix at different concentrations were examined in detail using transmission electron microscopy (TEM, Philips CM-20) and high resolution transmission electron microscopy (HREM, JEOL 3010 with 300 kV accelerating voltage). KEYENCE VHX-950F digital microscope equipped with a high-sensitivity, high-speed CMOS camera with a framerate of 50 frames/sec was used to evaluate the wear track profile of samples after the wear test. Depth composition images were obtained of the uneven surfaces by compiling images at different focal planes. X-ray diffraction (XRD) with parallel beam geometry and Cu Kα radiation using a Bruker AXS D8 Discover diffractometer equipped with Göbel-mirror and a scintillation detector has been used for phase identification. The crystalline size and amount in exiting the composites has been preceded based on a standard less quantitative analysis of the composites was performed using the Bruker Diffrac. EVA software based on the ICDD JCPDS 2003 data base. Standard less quantitative analysis method is based on the comparison of the peak intensities of the identified phases to the intensities of a corundum standard. Renishaw 1000 B micro-Raman spectrometer attached to a Leica DM/LM microscope was used to perform Raman spectra at room temperature in the wave number range of 150–3500 cm^{-1} with 488 nm laser excitation. The spectral resolution of the system is 2.5 $cm^{-1}$and the diameter of the excitation spot is 1 μm.

3. Results

3.1 Microstructure and mechanical properties

Structural investigations show that the powder morphology of pure 8YSZ (Fig. 1a) has been significantly modified to a refined and homogeneous microstructure sized of approximately 400 nm with soft grain edges that tends to form low-angle grain boundaries due to repeated welding, which was the aim of the milling. The further grain refinement is well recognized with MWCNT addition to 8YSZ matrix (Fig. 1b-d). The grain refinement increased proportionally with increasing of the MWCNT content.

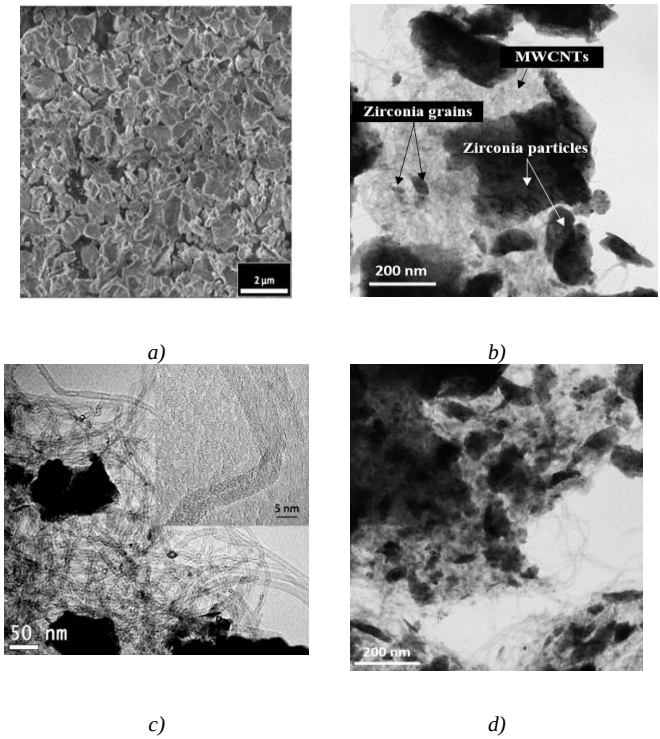

Fig. 1. *Structural study of 8YSZ / MWCNT powder mixture. a) SEM image of 8YSZ matrix after milling. b) TEM images of* ZR-1, *c)* ZR-5 *with detail of MWCNT and d)* ZR-10.

In case of 1 wt% addition, the MWCNTs were dispersed uniformly along the contact edges of 8YSZ grains, while the high MWCNT content (5 and 10 wt%) results in the formation of small zirconia grains of (< 100 nm) and particles (> 200 nm) embedded into MWCNTs agglomerations and networks. The detailed surface morphology observation revealed at first sight a smooth, homogeneous and tenacious surface for standalone 8YSZ (Fig. 2a). The surface area of ZR-1 composite, was mainly predominated by nanometric phases (dark spots) reflecting a good MWCNTs distribution in 8YSZ matrix and a high interfacial bonding resulting in a microstructure refinement (Fig. 2b). By contrast, it is most remarkable that the surface morphology of the 8YSZ containing highest amount of MWCNTs 10 wt% exhibits a reduced interfacial bonding between 8YSZ and MWCNTs, a deep superficial porosity and high agglomeration of MWCNTs (Fig. 2c).

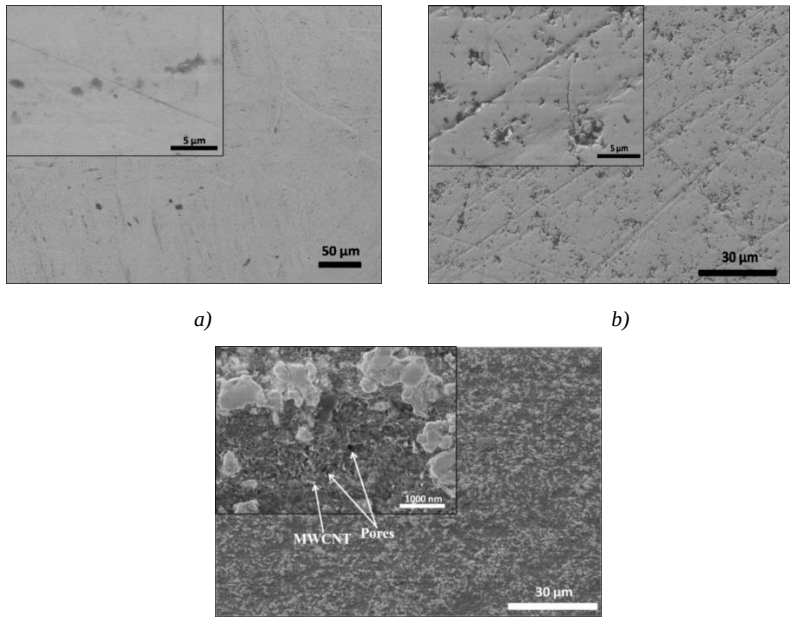

Fig. 2. *SEM images of the morphological differences between the sintered composites. a) ZR, b) ZR-1 and c) ZR-10.*

These effects led to form a rough surface and discontinuous 8YSZ particles embedded in a nanometer phase composed by MWCNTs agglomerations. The behaviour of zirconia matrix under a certain applied compressive load changed with the addition of MWCNTs. In fact, the matrix dissipates the applied stress to MWCNTs. This mechanism played an important role in improving the fracture toughness of the composites. MWCNT pulling-out, crack bridging, crack deflection and branching are among the typical phenomena resulting from toughening zirconia with MWCNTs. The properties of MWCNTs are considered as crucial factors that control the efficiency of stress transferred from the matrix to the fiber. The indentation and the crack propagation in the sintered composites at 1400 °C, have been carefully examined (Fig. 3). MWCNTs pulling-out and bridged region are visible in the 8YSZ composite reinforced with 1 wt% addition (Fig. 3b). Two interesting observations were noticed during the crack propagation analysis between the standalone matrix and the reinforced matrix with 1 wt% MWCNTs. Generally, the average crack path length calculated from the indentation center was more or less higher than that of the unreinforced matrix about ~ 50 µm via ~ 46 µm. This could be attributed to the residual porosity induced by the MWCNTs.

Further, the crack widths were narrowed to an average ~ 76 µm compared to that of the standalone matrix ~120 µm. Indeed, the observed bridged regions in the reinforced composite form an obstacle that protect the crack from reaching a critical state and consequently prone to failure. Thus, the crack path appears more restrained and tapered. Conversely, an inconsistent 8YSZ matrix was observed in the case of ZR-10 (Fig. 3c) which was attributed to discontinuity of zirconia particles and deep open porosity on surface. In case of ZR-5 and ZR-10, the dispersion of the stress occurs throughout the pores starting from the center of indentation and ending after a long unrestrained path. Thereby, this material exhibited low mechanical properties. Fig. 3d indicates the contribution of crack deflection and crack branching in the toughening mechanism for ZR-1 composite. It was assumed that crack deflection takes place when the crack tends to follow the grain boundaries and therefore reflects the composite microstructure. Tab.2 presents the mechanical and structural properties of the sintered 8YSZ / MWCNTs composites. The density and porosity measurements show a moderate improvement from 6.02 g/cm^3 to 6.76 g/cm^3 and remarkable reduction from 33 % to

16.5 % respectively in favor of ZR-1 composite compared to the ZR. Whereas, up to 5 wt% MWCNTs the density dropped to lower values and therefore the porosity followed inversely proportional trend. Fractographic test performed upon the sintered composite with 3-point bending test revealed a coarse microstructure with an average grain size of approximately 6.11 ± 4.08 μm, which is significantly higher than the recorded ones with added MWCNTs. The drastic reduction of the grain size has been observed in the structure of ZR-1 composite from 6.11 ± 4.08 μm to 0.96 ± 0.49 μm (Tab. 1). Hence, the well dispersed MWCNTs observed in ZR-1 composite led to the formation of an extra barrier to fracture propagation along the grain boundaries

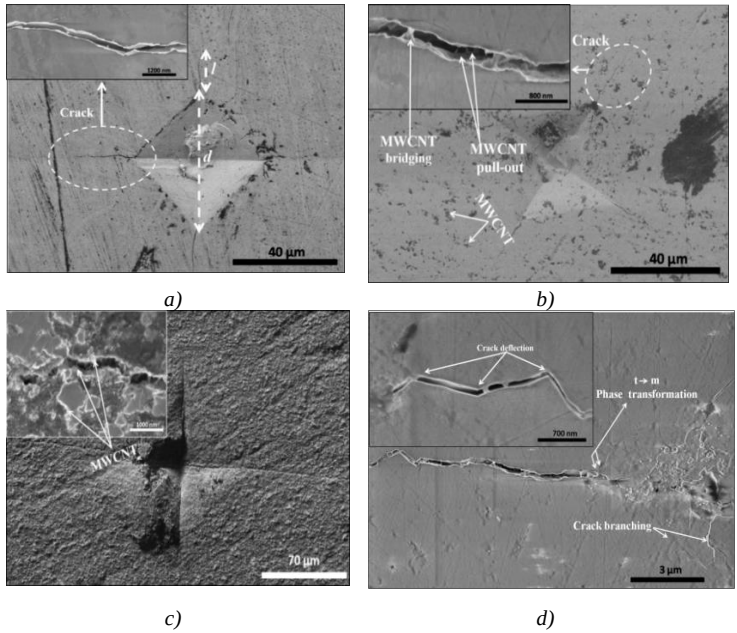

Fig. 3. *Crack patterns and indentation produced by Vickers hardness. a) ZR, b) ZR-1 and c) ZR-10. d) SEM image showing crack deflection, crack branching and the possibility of phase transformation occurrence (tetragonal to monoclinic) in ZR-1 composite.*

This behavior is reinforced by minimal apparent porosity (16.50 %). Furthermore, the microstructural modification was illustrated mainly by severe grain refinement 0.54 ± 0.04 µm in ZR-5 composite and 0.28 ± 0.01 µm in ZR-10 composite, simultaneously with the observation of a considerable increase in the residual porosity to 41.64 % via ZR-5 and to 46.28 % via ZR-10 resulting from inevitable agglomeration of higher amount of MWCNTs in matrix.

The flexural strength shows an increase in favor of ZR-1 compared to the monolithic material (ZR) from 464 MPa to 502 MPa. Meanwhile, ZR-5 and ZR-10 express typical brittle fracture confirmed by critical decline of the flexural strength to 263 MPa and 166 MPa respectively. The variation of Vickers hardness and indentation fracture toughness with surface displacement is practically homogenous and reached high values ∼13.49 GPa for 8YSZ ceramic and ∼12.44 GPa for 8YSZ containing 1 wt% of MWCNTs (Fig. 4a-b). The average hardness for composites decreased with increasing of MWCNT addition sharply to low values ∼5 GPa (ZR-5) and ∼ 2.7 GPa (ZR-10) successively besides exhibiting a fluctuated distribution, due to the non-homogeneity of Vickers hardness. The fracture toughness variation line of ZR-1 had initially an upward trend followed by a flat band region where the reference (ZR) was almost overlapping each other at an average ~ 3.2 MPa.m$^{0.5}$. On the other hand, the fracture toughness decreased rapidly to low values ∼1.5 MPa.m$^{0.5}$ and ∼ 1.3 MPa.m$^{0.5}$ when MWCNTs content has been increased to 5 wt% and 10 wt%, as well.

Tab. 2. *Mechanical and microstructural properties of sintered 8YSZ / MWCNTs composites.*

	Apparent porosity (%)	**Density (g/cm^3)**	**Average hardness (GPa)**	**Bending strength (MPa)**	**Average K_{Ic} (MPa·m$^{1/2}$)**	**Grain size (µm)**
ZR	32.99	6.02	13.49 ± 0.2	464	3.06 ± 0.22	6.11 ± 4.08
ZR-1	16.50	6.75	12.44 ± 0.9	502	2.63 ± 0.62	0.96 ± 0.49
ZR-5	41.64	4.97	5.07 ± 1.17	263	1.28 ± 0.42	0.54 ± 0.04
ZR-10	46.28	4.36	2.53 ± 0.76	166	1.30 ± 0.44	0.28 ± 0.01

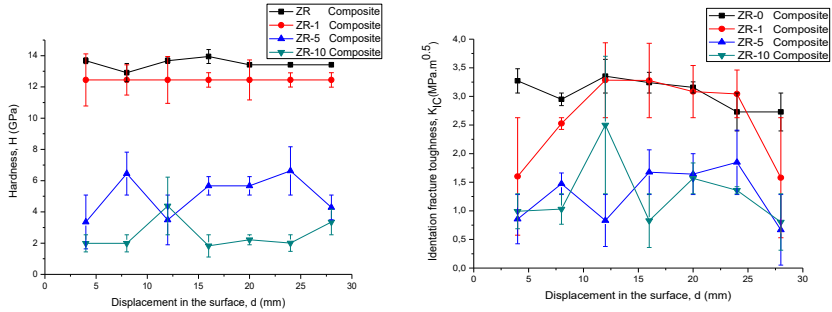

a) b)

Fig. 4. *Mechanical properties reference and different of 8YSZ / MWCNTs composites. a) Variation of Vickers hardness, b) Variation of indentation fracture toughness with surface displacement.*

3.2 Phase analysis

X-ray diffraction analysis was used to investigate and quantify the phase evolution and the corresponding crystal size in the sintered composites (Fig. 5). Tab.3 summarizes and quantifies the structural phase transition with the corresponding crystal size perceived in each composite according to MWCNTs content sintered at 1400 °C. Monolithic sintered composite reveled the formation of new phase (tetragonal) with high quantity (~ 75.2 %) via only a small fraction of cubic phase round 24.8 %.

Tab. 3. *Structural phases and crystal size parameters calculated with Standard less quantitative analysis method for ZR, ZR-1, ZR-5 and ZR-10 composites prepared by SPS at 1400°C.*

Sample	Cubic phase (%)	Cryst size (nm)	Tetragonal phase (%)	Cryst. size (nm)	Monoclinic phase (%)	Cryst. size (nm)
ZR	24.8	50.4	75.2	43.4	0	0
ZR-1	34.6	41.8	63.1	41.9	2.4	37.1
ZR-5	28.4	41.7	67.3	36.4	4.3	24.6
ZR-10	37.4	48.7	58.4	53.2	4.2	27.4

This fact illustrates a clear influence of sintering process by SPS at high temperature1400°C (Fig. 5a) to enhance the growth of tetragonal phase as compared with composites at powder state in which the dominant phase was mainly cubic (Fig. 5b). Indeed, the tetragonal phase has been retained to room temperature, thereby enhancing the comprehensive mechanical properties of these composites based on transformation toughening zirconia mechanism. On the other hand, the increased monoclinic phase in case of ZR-5 and ZR-10 composites is associated with tetragonal to monoclinic phase transformation occurrence during the cooling stage which is associated with large volume expansion promoting the risk of brittle failure.

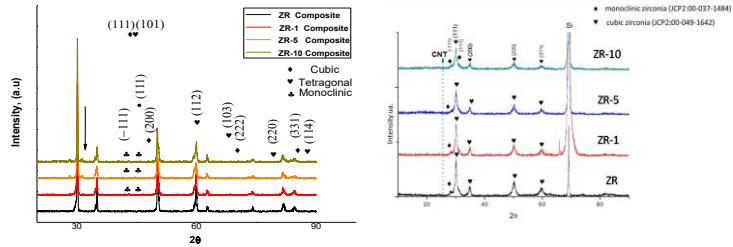

a) b)

Fig. 5. *XRD patterns of 8YSZ reference and 8YSZ / MWCNT. a) after sintering, b) after milling.*

3.3 Friction coefficient and wear rate

Fig. 6a presents the average friction coefficient (μ) corresponding to the sliding distance in the range of 0–40 m and 40–400 m of the sintered composites tested under V1 = 0.036 m/s, V2 = 0.11 m/s sliding speeds, using ball on disc method and Si_3N_4 balls counterpart. At low sliding speed (V1= 0.036 m/s) the average steady state friction coefficient (μ_{AFS}) is seen to be significantly high~0.76 and quit similar to all the tested composites regardless their specific micro-structural properties or MWCNTs content. However, the average steady state friction coefficient (μ_{AFS}) carried out at V2= 0.11 m/s sliding speed decreased in (μ_{AFS}) regarding the more brittle composites possessing lower grain size as well as mechanical properties (0.608 via ZR-5 and

0.649 via ZR-10). This draws an easier sliding between the rubbing surfaces and friction improvement. In fact, this friction improvement is shown to be linked with the apparition of intrinsic solid lubricant effect due to MWCNTs exfoliation (carbon peak decrease) and high Si incorporation as confirmed by EDS spectrum (not shown). The wear rate results at the speed of V1= 0.036 m/s, indicated 99.9 % improvement in the wear rate in case of 1 wt% MWCNTs followed by 95 % for 5 wt% and 64 % in the case of 10 wt% MWCNTs addition compared to pure 8YSZ (Fig. 6b). Applying high velocity (V2= 0.11m/s) resulted in a better wear resistance. In fact, the wear rate results were closely similar or occasionally high in all the composites, therefore the influence of structural properties was not recognized as MWCNTs content increased.

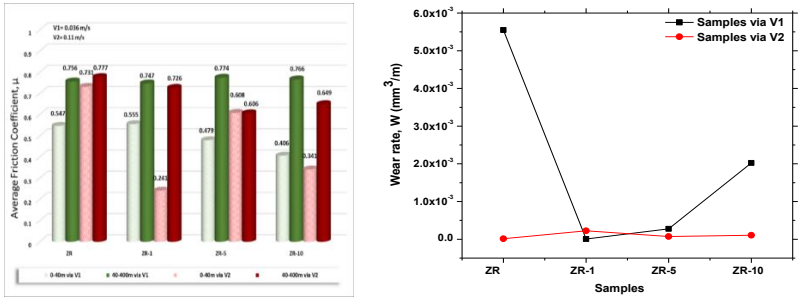

a) b)

Fig. 6. *Tribological properties of composites. a) Comparative graph presenting the Average friction coefficient (μ) during transitory state (0-40m) and steady state (40-400m) for all the composites tested at fix normal load (5N) and different sliding rates (V1=0.036 m/s, V2=0.11 m/s), b) wear rate.*

4. GENERAL CONCLUSION

Multiwall carbon nanotube (MWCNT) reinforced zirconia (ZrO_2) composites are attracting growing interest thanks to their ability of self-healing of the crack, the possibility to tailor the desired nanostructured properties and their outstanding wear behavior. The aim of my PhD work is the experimental synthesis of 8 mol% yttria stabilized zirconia (8YSZ) containing 1, 5 and 10 wt% MWCNTs. I also have aimed to

explore how the microstructure affect their mechanical and tribological properties. Thus, affording the possibility to extend their wide use in technical applications with excellent efficiency. The first part of my work was devoted to the investigations of the effect of the milling process performed at rotational speed of 4000 rpm and conducted for 5 h on the control of the grain size and morphology of MWCNT dispersion, homogeneity with respect to its concentration at powder state. I accomplished the initial characterization of the microstructure in 8YSZ / MWCNTs powder including MWCNTs agglomeration and MWCNTs fiber structural features. I found that the powder morphology of pure 8YSZ has been significantly modified after milling to a refined and homogeneous microstructure sized of approximately 400 nm with soft grain edges, which tends to form low-angle grain boundaries due to repeated welding. Further 8YSZ grain refinement and MWCNT bundles have been recorded to increase proportionally with MWCNT content, while the later showed practically nondestructive structural milling. The addition of 1 wt% MWCNTs led to uniform dispersion of MWCNT fibers along the contact edges of 8YSZ grains. In the second part of my PhD work, the microstructural features namely density, porosity, grain growth and phases of the sintered 8YSZ / MWCNT composites by spark plasma sintering (SPS) process at 1400 °C have been subjected to a detailed investigation and connected with the results from Vickers hardness and indentation fracture toughness measurements. In fact, 8YSZ / 1 wt% MWCNTs sintered composite owns the highest density 6.76 g/cm3 and bending strength of 502 MPa besides the lowest porosity of 16.5 % among all the tested composites. I explain it with several factors mainly: 1. the effect of sintering process at 1400 °C which allowed the suppression of the minor agglomerations reported in the milled composites powder;2. the optimum MWCNT concentration of 1 wt% enabled an average grain refinement to 0.96 ± 0.49 μm as well as high interfacial bonding between the grains. Furthermore, the analysis of the crack propagation modes showed the presence of MWCNT pull-out, crack bridging and crack deflections besides more restrained and tapered crack path in the 8YSZ /1 wt% composite compared to the reference. I showed that these toughening mechanisms played a vital role in enhancing the resistance to crack propagation. Quantitative X-rays measurements indicated the presence of considerable tetragonal phase at room temperature in the sintered composites with different proportions, unlike the composites powder in which the cubic phase was dominant. The highest proportion of tetragonal phase was obtained in the monolithic composites. This fact leads to enhanced Vickers

hardness values (average ~13.49 GPa) due to the intrinsic property of transformation toughening zirconia. On the other hand, high degradation of the mechanical and Indentation Fracture Toughness was well approved in case of 5 wt% and 10 wt% MWCNTs addition. This was associated with incoherent and discontinuous matrix, reduced interfacial bonding due to the deep open pores on the surface which caused a long unrestrained crack path.

In the last part of my work, I investigated the influence of sliding speed on the tribological properties using Si_3N_4 balls, dry sliding conditions, low (V1= 0.036 m/s) and high (V2= 0.11 m/s) speed values. Outstanding wear improvement at both low/high sliding speed has been reported in case of 1 wt% of MWCNTs. This was most likely attributed to two main factors: 1. the formation of a perfectly continuous and uniform tribofilm; 2. the improved flexural strength and density. I developed the new interpretation of the observed wear mechanism in the studied 8YSZ ceramic composites with respect to MWCNTs content based on a comparative characterization performed inside and outside the wear track using SEM and EDS. Further, the steady state friction coefficient marked significant decrease at high sliding speed with 5 wt% and 10 wt% of MWCNTs content.

5. Thesis of PhD work

The current investigation resulted into the novel founding summarized as follow:

1. **I showed that the attrition milling and spark plasma sintering are appropriate technologies for production of well densified MWCNTs reinforced 8YSZ composites**. I proved that the optimized wet milling conditions (4000 rotational speed for 5 hours, in ethanol) and sintering parameters (1400 °C, uniaxial pressure of 50 MPa, dwell time of 5 min, in vacuum) are needed to achieve non-destructive MWCNT fibers in composites and to maintain the MWCNTs during the all steps of preparation process [1, 2].

2. **I proved that the structural properties of final sintered composites are dependent on the amount of MWCNTs addition.** The increasing of MWCNTs content from 1 wt% to 10 wt% led to a proportional grain refinement and to the formation of MWCNTs agglomeration.

I proved that the increasing MWCNTs addition resulted in a microstructure consisting of cubic zirconia (~33%), lower amount of monoclinic (m) (~3.5%) and higher amount of tetragonal phase (63.5%) considering the average values of ceramic phases. This fact demonstrates the role of MWCNTs addition to successfully synthesis metastable tetragonal (t) phase and to reduce t→m phase transformation during cooling stage of sintering [2].

3. **I proved that only 1 wt% MWCNT addition improved the mechanical properties of final composites**. I found that the hardness and indentation fracture toughness were mostly equal with reference, while the bending strength increased for 1 w% MWCNTs content. The structural factors responsible for this improvement are the good distribution of MWCNTs in ceramic matrix, the grain refinement to $0.96 \pm 0.49\mu m$ and high interfacial bonding among the grains resulting from the dominating transgranular fracture mode. In the case of 5 and 10 wt% MWCNTs addition, hardness and indentation fracture toughness showed lower values and fluctuated distribution characterized by intergranular fracture mode [2].

4. **I developed a novel interpretation of the observed wear mechanism in the zirconia ceramic composites with respect to MWCNTs content based on a comparative characterization performed inside and outside the wear track.** I showed an outstanding wear improvement of composite with 1 wt% MWCNTs at low (0.036 m/s) and high (0.11 m/s) sliding speeds attributed to the formation of a perfectly continuous, uniform tribofilm and the improved bending strength and density. Further, the steady state friction coefficient marked significant decrease at higher sliding speed with 5 and 10 wt% of MWCNTs content. In fact, this finding was mainly linked with intrinsic lubricant effect due to MWCNT exfoliation and the formation of a thick and dense tribofilm [3].

6. Publications

6.1 Publications related to the thesis

[1] **S. Lamnini,** Z. Fogarassy, Z.E. Horváth, S. Tóth, K. Balázsi, C. Balázsi, The role of the attrition milling on the grain size and distribution of the carbon nanotubes in YSZ powders, Bol. La Soc. Esp. Ceram. y Vidr. (2018) 126 - 133 (IF 1.633).

[2] **S. Lamnini**, Z. Károly, E. Bódis, K. Balázsi, C. Balázsi, Influence of structure on the hardness and the toughening mechanism of the sintered 8YSZ/MWCNTs composites, Ceram. Int. 45:4 (2019) 5058 - 5065 (IF 3.450).

[3] **S. Lamnini**, C. Balázsi, K. Balázsi, Wear mechanism of spark plasma sintered MWCNTs reinforced zirconia composites under dry sliding conditions, Wear. 430–431 (2019) 280-281 (IF 2.950).

6.2 Other publications

[4] **S. Lamnini**, P. Kádár, Survey on perspectives of PV technology and their applications. SAMI 2017 - IEEE 15th Int. Symp. Appl. Mach. Intell. Informatics, Proc., 2017.

6.3 Conferences

S. Lamnini, P. Kádár, Sami 2017Conference, 15th International Symposium on Applied Machine Intelligence and Informatics, 2017, January 26-28, Herlany, Slovakia. (Poster presentation)

S. Lamnini, Z. Fogarassy, Z.E. Horváth, K. Balazsi, C. Balazsi, ECerS 2017, 15th Conference & Exhibition of the European Ceramic Society, 2017, Július7-13, Budapest. (Poster presentation)

S. Lamnini, Z. Fogarassy, Z.E. Horváth, K. Balazsi, C. Balazsi, FEMS Junior EUROMAT 2018, The main Event for Young Material Scientists,2018, July8-12, Budapest. (Oral presentation)

S. Lamnini, Student speech context participation,16th Conference & Exhibition of the European Ceramic Society, 2019, June 16-20, Torino, Italy. (Oral presentation)

S. Lamnini, Z. Fogarassy, Z.E. Horváth, K. Balazsi, C. Balazsi, Woceram 2019, International workshop on Women in ceramic science, 2019, April 7-9, Budapest. (Oral presentation)

S. Lamnini, K. Balazsi, C. Balazsi, 1st"Fine ceramics day" event of Hungarian Scientific Society of Silicate Industry, 2018, 9 April, MTA EK, Budapest, Hungary. (Oral presentation)
S. Lamnini, Z. Károly, E. Bódis, K. Balázsi, C. Balázsi, 2nd "Fine ceramics day" event of Hungarian Scientific Society of Silicate Industry, 2019, 193March, Budapest, Hungary. (Oral presentation)
S. Lamnini, Z. Fogarassy, Z.E. Horváth, K. Balazsi, C. Balazsi, 44th International Conference & Exposition on Advanced Ceramics & Composites (ICACC) and ACerS Winter workshop 2020, Jan 26–31, 2020, in Daytona Beach, Florida. (Poster presentation)

7. Scientific Parameters

All Publications: 4	Publications related to PhD work: 3
Cumulative impact Factor: 8.033	Impact factors related to PhD work: 8.033
All Citations: 8	Citations related to PhD work: 5